^{57}Fe NMR and relaxation by strong collision in the tunneling regime in the molecular nanomagnet Fe8

S. H. Baek,[1,*] F. Borsa,[1,2] Y. Furukawa,[3] Y. Hatanaka,[3] S. Kawakami,[3] K. Kumagai,[3] B. J. Suh,[1,4] and A. Cornia[5]

[1]*Department of Physics and Astronomy, Iowa State University and Ames Laboratory, Ames, Iowa 50011, USA*
[2]*Dipartimento di Fisica "A Volta" e Unita'INFM di Pavia, via Bassi 6, 271000 Pavia, Italy*
[3]*Department of Physics, Faculty of Science, Hokkaido University, Sapporo, 060-0810 Japan*
[4]*Department of Physics, Catholic University of Korea, Puchon, 420-473, Korea*
[5]*Dipartimento di Chimica-Centro SCS, Università di Modena e Reggio Emilia, UdR INSTM, I-41100, Modena, Italy*
(Received 15 February 2005; published 30 June 2005)

^{57}Fe NMR measurements have been performed in single crystal and oriented powder of enriched ^{57}Fe8 molecular cluster in the temperature range 0.05–1.7 K in zero external field and with small perturbing field up to 1 T for both transverse and longitudinal orientation of H with respect to the anisotropy axis. The ^{57}Fe NMR spectrum is analyzed in terms of a dominant contribution due to the hyperfine interaction arising from core polarization. The measured temperature dependence of the resonance frequency is explained well by calculating the local average magnetic moment of the Fe^{3+} ion with a simple model which incorporates the effects of thermal average in the low lying energy states. Nuclear spin-lattice relaxation rate $(1/T_1)$ and spin-spin relaxation rate $(1/T_2)$ were investigated via temperature and field dependences. The obtained results are analyzed in terms of both intrawell thermal fluctuations of the hyperfine fields due to spin-phonon interaction, and interwell fluctuations due to phonon assisted quantum tunneling of the magnetization. It is argued that in zero external field and at low T the ^{57}Fe and the proton $1/T_1$ is dominated by a strong collision relaxation mechanism due to the fact that phonon assisted tunneling transitions generate a sudden reversal of the local quantization field at the nuclear site. The data could be explained satisfactorily by assuming that the ^{57}Fe $1/T_1$ measures directly the effective tunneling rate. However, in order to fit the data we had to assume a larger in-plane anisotropy than previously reported, resulting in a bigger tunneling splitting in zero field. A comparison with published data of ^{55}Mn in Mn12 indicates that a strong collision relaxation mechanism may apply also in Mn12. Finally the H and T dependence of ^{57}Fe $1/T_2$ is well explained simply in terms of thermal fluctuations of the magnetization without any tunneling contribution. At very low T the $1/T_2$ approaches a limiting value which can be explained in terms of the dipolar interaction between proton and ^{57}Fe nuclei in the quasistatic regime.

I. INTRODUCTION

Single molecule magnets (SMM) are magnetic systems formed by a cluster of transition metal ions within large organic molecules.[1–3] SMM are characterized by nearly identical and magnetically isolated molecules with negligible intermolecular magnetic interactions, which allows the investigation of nanomagnetism from the macroscopic measurement of the bulk sample. Recently, SMM have been paid much attention not only for the fundamental physical properties but also for the potential applications in quantum computing and data storage.[4] Among the molecular magnets, Mn12ac and Fe8 clusters,[5,6] which have a high total ground state spin $(S=10)$ and a large uniaxial anisotropy, are of particular interest due to the superparamagnetic behavior and the quantum tunneling of the magnetization (QTM) observed at low temperature.[7–9]

The octanuclear Fe^{3+} cluster[10] (Fe8) is a particularly good candidate for the study of quantum effects since it couples an uniaxial anisotropy leading to an energy barrier[5] of ~25 K to a non-negligible in-plane anisotropy. The latter is crucial in enhancing the tunneling splitting of the pairwise degenerate magnetic quantum states. In fact, Fe8 shows pure quantum regime below 0.4 K and periodic oscillations of the tunnel splitting interpreted in terms of Berry phase.[11–13] Moreover, it was found that the enrichment of ^{57}Fe isotope in Fe8 shortens the relaxation time demonstrating that the hyperfine field plays a key part in QTM.[14] Together with intensive theoretical investigations,[15–19] QTM in Fe8 has been revealed by various techniques such as magnetization measurements,[12,13] ac-susceptibility,[5,20] specific heat measurement,[21,22] high-frequency resonant experiments,[23] circularly polarized microwave technique,[24] and nuclear magnetic resonance.[25,26]

Nuclear magnetic resonance (NMR) has proved to be a powerful tool to investigate the local properties of magnetic systems because the nuclear spin is very sensitive to local fields and thus provides valuable information on spin dynamics. Several proton NMR studies on Fe8 have been already performed yielding information about hyperfine interaction, fluctuations of the local moments of Fe^{3+} ions,[27] and tunneling effects.[25,26,28] In proton NMR, however, we can obtain only indirect information due to an averaging effect arising from the wide distribution of protons in each molecule and the weak hyperfine coupling between Fe^{3+} moments and protons mostly of dipolar origin.

^{57}Fe nucleus is, in principle, a much better probe than proton since it couples directly to the magnetic electrons of the Fe^{3+} ions with a strong hyperfine field which allows the

investigation of ^{57}Fe NMR in zero external field. The only drawback is that the strong coupling makes the NMR signal detectable only in a narrow temperature range. Previous ^{57}Fe NMR studies have yielded direct information on the local magnetic structure of the ground state and the hyperfine interactions.[29,30] In addition to the static effects mentioned above, ^{57}Fe NMR can provide precious information about the dynamic magnetic properties, including the tunneling effect, through the measurements of the relaxation rates as a function of temperature and external field, and by the temperature dependence of the resonance frequency in zero field, which are the subjects of the present investigation.

In this paper, we report ^{57}Fe NMR measurements in a sample of oriented powder and in a single crystal both enriched in the ^{57}Fe isotope. In Sec. II, the sample properties and some experimental details are illustrated. After presenting the experimental results in Sec. III, the hyperfine interactions and static magnetic properties are summarized in Sec. IV with emphasis on the data on the temperature dependence of the nuclear resonance frequency in zero field. In Sec. V we discuss and deduce theoretical spin dynamics models for the nuclear relaxation rates in the low temperature region. A central result of the present investigation is the observation of a strong collision relaxation mechanism for both protons and ^{57}Fe zero field NMR in the tunneling regime, a rarely observed situation in nuclear spin lattice relaxation due to magnetic interactions. Detailed comparison of the data of the relaxation rates with the theoretical models proposed in Sec. V are reported in Sec. VI. Also the relaxation rates of ^{55}Mn are compared with those of ^{57}Fe. In Sec. VII, our experimental results and theoretical analysis are summarized.

II. SAMPLE PROPERTIES AND EXPERIMENTAL DETAILS

The formula of the molecular cluster is $[Fe_8(tacn)_6O_2(OH)_{12}]^{8+}[Br_8 \cdot 9H_2O]^{8-}$ (in short Fe8) where tacn is the organic ligand 1,4,7-triazacyclonane and the ionic charge 8+ of the cation is compensated by seven bound Br^- ions and one Br^- counterion. Fe8 consists of eight Fe^{3+} ions ($s=5/2$) where the Fe ions are coupled together by 12 μ_3-oxo and μ_2-hydroxo bridges through different exchange pathways resulting in well-known butterfly configuration. The magnetic properties of Fe8 at low temperatures are characterized by a total spin of $S=10$ for each molecule resulting from competing nearest neighbor antiferromagnetic interactions between the Fe^{3+} ions.[31]

The $S=10$ magnetic ground state of the Fe8 molecular cluster can be described by a total spin model Hamiltonian,

$$\mathcal{H} = DS_z^2 + E(S_x^2 - S_y^2) + g\mu_B \mathbf{S} \cdot \mathbf{H}, \qquad (1)$$

where z is the direction of the large uniaxial anisotropy, S_x, S_y, and S_z are the three components of the total spin operator, D and E are the axial and the rhombic anisotropy parameter, respectively, μ_B is the Bohr magneton, and the last term of the Hamiltonian describes the Zeeman energy associated with an applied field H. The crystal structure of Fe8 is shown
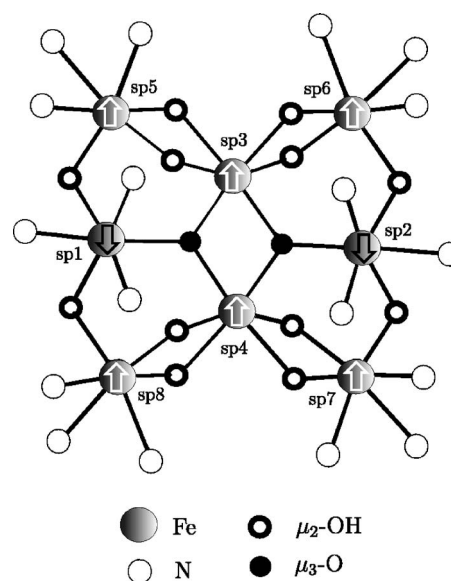
FIG. 1. Schematic diagram of Fe8 molecular cluster. The arrows represent ionic spin direction of Fe^{3+} ion with $s=5/2$ in $S=10$ ground state.

in Fig. 1. The arrows represent the spin structure of Fe^{3+} ions in the ground state $S=10$.

In order to synthesize the ^{57}Fe-enriched Fe8 cluster, 95% enriched ^{57}Fe foil (53.3 mg, 0.936 mmol) was carefully dissolved in 400 mL of a $3:1$ (v/v) mixture of concentrated HCl and HNO_3 in a Kjeldahl flask. The solution was boiled and HCl added dropwise to keep the volume constant until evolution of brown NO_2 fumes ceased. To the cool concentrated solution excess thionyl chloride was added dropwise (Caution, vigorous evolution of SO2 and HCl) and the unreacted portion was distilled off under nitrogen. The black lustrous $FeCl_3$ residue was dissolved in methanol (4 mL) and treated with a solution of tacn112 mg, 0.867 mmol) in methanol (1 mL) with stirring. Yellow $[^{57}Fe(tacn)Cl_3]$ was collected by filtration, washed with ethanol (1.5 mL) and dried under vacuum (194 mg, 76% yield). The solid was dissolved in 15 mL of water containing 1.5 mL of pyridine and the solution was stirred for 1 h before addition of NaBr (3.9 g). After additional 10 minutes of stirring, any undissolved material was removed by centrifugation and the clear solution was left undisturbed in a desiccator at reduced pressure (300–350 mm Hg) over P_2O_5 for 2–3 weeks. Crystalline ^{57}Fe8 (126 mg, 67% yield) was collected by filtration and dried by N_2 before measurement. The oriented-powder sample of Fe8 has been prepared by mixing the powdered material with epoxy (EpoTech 301) and letting it set in a magnetic field of 7.2 T at room temperature for 12 hours. The sample filling factor is about 20%–30% out of the volume of a cylinder with 5 mm diameter and 20 mm length. Orienting the powder sample results in a better signal to noise ratio and a narrow signal even in zero magnetic field due to the orientation of the grains with respect to the radio frequency magnetic field. We also succeeded in making a single crystal of ^{57}Fe8 which was used to investigate the relaxation measurements at very low temperatures.

The ^{57}Fe ($I=1/2$) NMR measurements were performed using TecMag Fourier Transform (FT) pulse spectrometer. A
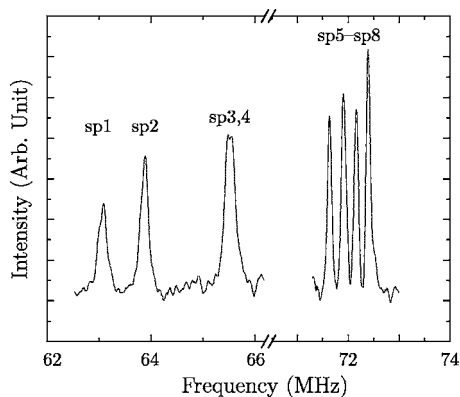
FIG. 2. The ^{57}Fe NMR spectra in zero field. Each line is labeled with $sp1-sp8$ (see Table I).

($\pi/2-\pi$) pulse sequence (Hahn echo) has been used for the measurements with $1.5-3$ μs $\pi/2$ pulse length and $8-12$ μs separation between pulses depending on the spectrometer and experimental conditions. The $sp8$ NMR line was saturated with the comb pulse train with 10 pulses for the measurement of T_1 and the obtained recovery data with variable delays were fitted to the single exponential recovery law. The T_2 data were obtained from an exponential fit of the decay of the echo signal as a function of pulse spacing. The experiment has been carried out in the temperature range of $0.05-1.7$ K by using a closed cycle ^{3}He cryostat and a ^{3}He—^{4}He dilution refrigerator cryostat in the external fields of $0-1$ T.

III. EXPERIMENTAL RESULTS

A. Zero field ^{57}Fe NMR spectrum

The zero-field ^{57}Fe NMR spectra in Fe8 at 1.5 K has been reported previously with the analysis of the field dependence of the NMR lines for both longitudinal and transverse directions.[29,30] A fine structure of the spectra was observed from the narrow NMR lines as shown in Fig. 2. It has been confirmed that a quadruplet at higher frequency results from the four Fe lateral sites, a doublet at intermediate frequency from the two central sites and a second doublet at lower frequency from the two apical sites. Hereafter, we refer to each line as $sp1-sp8$ from low frequency to high frequency and in Fig. 1 the Fe^{3+} ion site associated with each NMR line is labeled accordingly. The experimental results are summarized in Table I.

The measurements of the temperature dependence of the resonance frequency $\nu(T)$ and of the ^{57}Fe nuclear spin-lattice relaxation rate reported in this paper refer only to the line $sp8$ in the spectrum for oriented powder and $sp4$ in single crystal (see Fig. 2 and Table I). This is sufficient for the purpose of studying the relative variations of the hyperfine fields and for the study of the spin dynamics. For confirmation $1/T_1$ has been measured at 1.5 K for each the eight NMR lines in the ^{57}Fe spectrum and the results were found to be within the same 10% error. It is noted that the nuclear dipolar interaction among the eight ^{57}Fe nuclei within each molecule is totally negligible and thus no spectral diffusion

TABLE I. NMR resonance frequencies and corresponding effective local fields obtained at 1.5 K in zero field.

Nuclear site	Frequency (MHz)	H_{eff} (T)
$sp1$	63.09	45.86
$sp2$	63.89	46.44
$sp3$	65.46	47.58
$sp4$	65.55	47.65
$sp5$	71.63	52.07
$sp6$	71.90	52.26
$sp7$	72.16	52.45
$sp8$	72.39	52.62

takes place among different lines in the NMR spectrum shown in Fig. 2.

The temperature dependence of the resonance frequency, $\nu(T)$, in zero field in the temperature range $0.5-1.7$ K is shown in Fig. 3. Above 1.7 K, the signal is not detectable due to the very short nuclear spin-spin relaxation time, T_2, as explained in details in the next section. The nuclear Larmor frequency decreases gradually as the temperature increases and it drops rapidly above 1.5 K when the signal becomes undetectable. The behavior of the temperature dependence of $\nu(T)$ in Fig. 3 can be ascribed to the reduction of average total spin moment, $\langle S \rangle$, due to the change in the thermal population of the magnetic sublevels. The limiting value of $\nu(T)$ as $T \to 0$ corresponds to the hyperfine field when the Fe8 molecules occupy the $m = \pm 10$ ground state.

B. Nuclear relaxation rates

The measurements of relaxation rates of ^{57}Fe were performed in the temperature range $0.05-1.7$ K at zero field for the temperature dependence, and in the field range $0-1$ T at 1.35 K for the field dependences. The temperature dependence of $1/T_1$ in zero field is shown in Fig. 4. $1/T_1$ shows fast decrease with decreasing temperature as it is expected due to the reduction of the thermal fluctuations of the hyper-
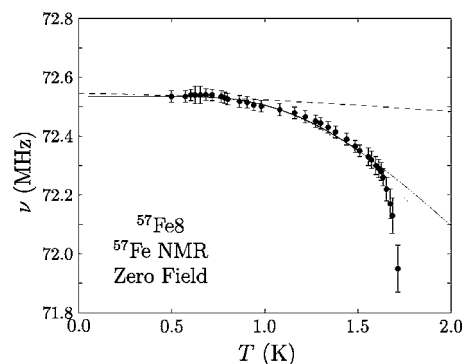
FIG. 3. Temperature dependence of resonance frequency of $sp8$ NMR line. Theoretical curves were obtained from Eq. (2) considering the two lowest levels (solid line) and all levels up to $m = \pm 5$ (dotted line). Bloch $T^{3/2}$ law (dashed line) is drawn for the comparison.
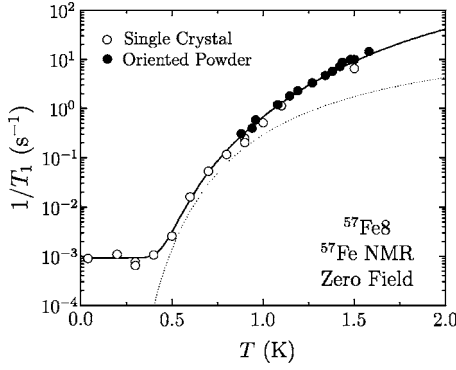
FIG. 4. Temperature dependence of $1/T_1$. Theoretical curves are given by Eq. (11) (dotted line) and the additional contribution is fitted well by adding Eq. (16) to Eq. (11) (solid line) with the appropriate choice of the parameters (see text).

fine fields. When a longitudinal field is applied, a fast drop of $1/T_1$ appears at very low fields, while for higher fields $1/T_1$ decreases monotonically with increasing field at a much slower rate as shown in Fig. 5. On the other hand, as it is shown in Fig. 6, $1/T_1$ in a transverse field increases rapidly at low fields and more slowly at higher fields. In the field range 1–2.5 T, the weak ^{57}Fe NMR signal cannot be measured since it overlaps with the much stronger signal from ^{1}H NMR. Due to the strength of the proton signal and its considerable width, the field range of overlap is very wide.

The longitudinal and transverse field dependences of $1/T_2$ are shown in Fig. 7. The temperature dependence of nuclear spin-spin relaxation rate ($1/T_2$) is very similar to one of $1/T_1$ although the magnitudes of the two relaxation rates differ by more than three orders of magnitude as shown in Fig. 8. When T is about 1.7 K the value of $1/T_2$ is about 10^5 s^{-1}, which is close to the limit of signal detectability in our spectrometer explaining the disappearance of the signal above 1.7 K. The measured T_2 is much shorter than the value ex-
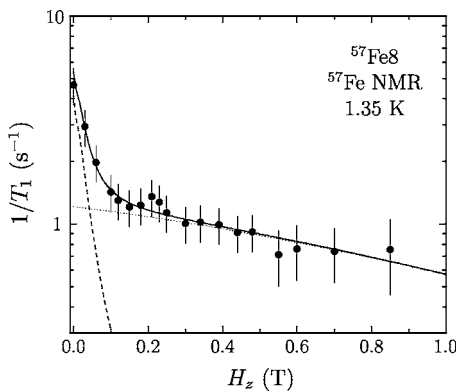
FIG. 5. Longitudinal field dependence of $1/T_1$ in oriented powder of Fe8. Dashed line is from Eqs. (16) and (18), dotted line is from Eq. (11), and solid line is the sum of the two contributions. The small enhancement at 0.22 T should be attributed to the level crossing between $m=+10$ and $m=-9$ where the tunneling rate increases as the result of the pairwise degeneracy of the excited states. The small enhancement at 0.22 T should be attributed to the level crossing between $m=+10$ and $m=-9$ where the tunneling rate increases as the result of the pairwise degeneracy of the excited states.
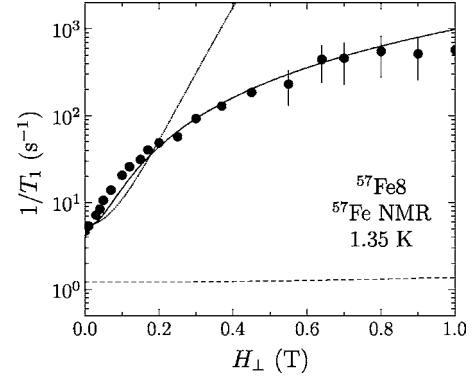
FIG. 6. Transverse field dependence of $1/T_1$. Dashed line represents spin-phonon contribution only [Eq. (11)], dotted line is the result of the calculation of the tunneling contribution without misalignment of the sample, and solid line is from the canting effect together with weak contributions from the thermal and the tunneling fluctuations [Eq. (20)].

pected for nuclear dipolar interaction in the intermediate temperature range 1–1.7 K (see the discussion in Sec. VI B 2). This circumstance together with the strong temperature dependence indicates that $1/T_2$ is driven by the slow dynamics of a strong hyperfine interaction above 1 K. In the proton case, since the ^{1}H zero field NMR spectrum is structured in a complex way, measurements at different positions of the spectrum were performed namely at 23 MHz and 18 MHz. The temperature dependence of ^{1}H $1/T_1$ are similar to the ones of ^{57}Fe $1/T_1$ as shown in Fig. 9.

IV. HYPERFINE INTERACTIONS AND STATIC MAGNETIC PROPERTIES

A. Hyperfine interactions

The hyperfine interactions in Fe8 have been analyzed in Refs. 29 and 30. By summarizing the previous analysis, the hyperfine field at the Fe^{3+} nuclear sites arises mainly from core polarization of inner s electrons due to $3d$ electrons. However, the experimental values are smaller than the theo-
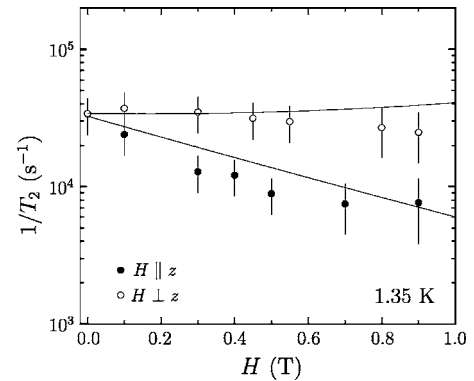
FIG. 7. Field dependences of $1/T_2$ for both longitudinal and transverse directions. Theoretical curves were obtained from Eq. (12) with $\gamma_N h_z = 2 \times 10^7$ (rad Hz). It appears that the tunneling and the canting effects do not contribute to $1/T_2$.
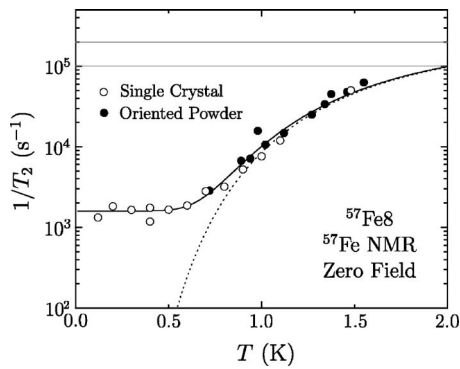
FIG. 8. Temperature dependence of $1/T_2$. Dotted line was obtained from Eq. (12) with $\gamma_N h_z = 2 \times 10^7$ (rad Hz) and solid line was obtained adding the constant value 1.6×10^3 s^{-1}, which is ascribed to the nuclear dipole-dipole interaction between ^{57}Fe and ^{1}H nuclei, to Eq. (12). The horizontal lines indicate the range of T_2 values above which the echo signal becomes undetectable depending on the spectrometer used and the experimental conditions.

retical value[32] which is estimated to be 62 T (see Table I) indicating that there is strong reduction of the local hyperfine field at the nuclear sites. The dipolar hyperfine field is normally zero in orbital singlet state like $3d^5$ configuration. But if Fe^{3+} ions in Fe8 do not have pure $3d^5$ configuration, the dipolar term could be non-negligible. One can make a qualitative estimate of the dipolar contribution from quadrupole splitting, Δ_Q, in Mössbauer spectroscopy using the fact that Δ_Q arises from an aspherical distribution of electrons in the valence orbitals and an aspherical charge distribution in the ligand sphere and/or lattice surroundings with symmetry lower than cubic.[33] The small values of Δ_Q 0.13, −0.11, and 0.057 mm/s, respectively, in Ref. 34 leads to the conclusion that the dipolar term would be too small to contribute to the main reduction of the local hyperfine fields but could contribute to the fine splitting of the lines in each Fe group. Therefore, the reduction of the local fields is attributed to the covalent bonds of Fe^{3+} ions with neighboring ligands. Since the covalency can result in both delocalization of 3d electrons and 4s hybridization, one can describe the configura-
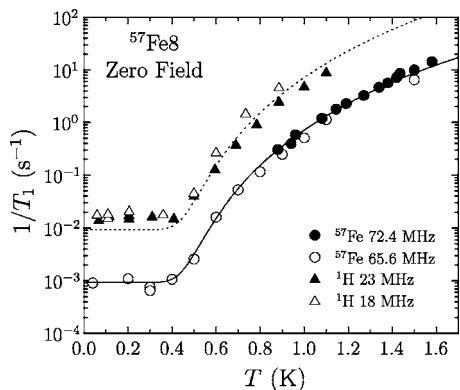
FIG. 9. Comparison of temperature dependence of ^{57}Fe $1/T_1$ with ^{1}H $1/T_1$ at zero field in Fe8. The full line is the same as in Fig. 1. The dotted line is the full line multiplied by 10. It is noted that the results for both ^{1}H and ^{57}Fe are independent of the Larmor frequency ω_L in agreement with Eq. (16).

tion of the magnetic electron in the covalent bond as $3d^{5-x}4s^y$. From the comparison of isomer shift values in Mössbauer spectroscopy[34] to the relation between isomer shift and partially occupied 4s orbitals by Walker et al.[35] we estimated $y \lesssim 0.05$. If we consider only the delocalization of 3d electrons, we get $x = 0.75$ for $sp1$ and $sp2$, 1.16 for $sp3$ and $sp4$, and 1.3 for $sp5 - sp8$ from the comparison of the experimental hyperfine field and the theoretical value of 62 T.[29] The above values for x should be viewed as upper limits since part of the reduction of the negative core polarization field can arise from the positive contact hyperfine field due to the 4s hybridization y.

B. Reduction of the hyperfine field due to thermal excitations

As seen in the preceding section the dominant contribution to the hyperfine field originates from contact interaction via a core polarization mechanism. Therefore we can assume that the resonance frequency is simply proportional to the average local spin moment in the Fe^{3+} ion, i.e., $\nu = A\langle s \rangle$. The reduction of the resonance frequency can arise either from a decrease with temperature of the hyperfine coupling constant A or from a reduction of the average spin moment due to thermal fluctuations. Since the temperature dependence of A is negligible at low temperature[36] the reduction of the hyperfine field is a direct measure of the reduction of the local magnetization. Since the average local spin moment $\langle s \rangle$ is proportional to the average total moment $\langle S \rangle$ of the molecule, we express $\nu(T)$ as a statistical average of the total magnetic moment of the molecule on the basis that the average total moment is reduced by thermal excitations from the magnetic ground state $m = \pm 10$ to excited states,

$$\frac{\nu(T)}{\nu(0)} = \frac{\langle S \rangle}{\langle S \rangle_{T=0}} = \frac{1}{\langle S \rangle_{T=0}} \left(\frac{\sum_m |m| \exp(-E_m/T)}{Z} \right), \quad (2)$$

where E_m is the energy of mth sublevel of $S = 10$ and Z is the partition function. We assume that the magnitude of the spin moment of a mth state corresponds to the value projected into quantization axis, e.g., 0.9 for $m = \pm 9$ state. Although this approach is based on a semiclassical picture of the spin, it provides a very successful theoretical curve. The result is shown in Fig. 3. The theoretical curve, however, depends strongly on the choice of D and E values in the Hamiltonian, Eq. (1). So far the values of D, −0.295, −0.276, and −0.293 K, and E, 0.055, 0.035, and 0.047 K have been reported by EPR,[37] magnetization measurements,[28] and neutron spectroscopy,[38] respectively. In our calculation, the best agreement is found for the choice of the parameters reported in Ref. 38 ($D = -0.293$ K and $E = 0.047$ K). In this report, these values of D and E are used in all theoretical calculations.

The three curves in Fig. 3 were obtained considering (i) Bloch $T^{3/2}$ law[39] (dashed line), (ii) Eq. (2) with only two lowest sublevels ($m = \pm 10$ and $m = \pm 9$) (solid line), (iii) Eq. (2) with all levels up to $m = \pm 5$ (dotted line).[40,63] As expected, the Bloch $T^{3/2}$ law based on spin wave theory does not apply to nanosize molecular magnets.[41,64] The agreement with the cases (ii) and (iii) is quite good with the exception

of the last higher temperature three points. Those points are affected by a large error because the signal becomes very weak due to the shortening of T_2 (see Sec. V). Thus it cannot be established for sure if the resonance frequency starts to drop rapidly at $T > 1.6$K. The drop could indeed take place if higher order states are included for higher temperature.

V. SPIN DYNAMICS

A. Nuclear relaxation due to thermal fluctuations

In this paragraph we consider the case of nuclear relaxation due to the changes of hyperfine field resulting from the transitions of the molecule from the $m = \pm 10$ ground state to excited states. In spite of the fact that the "lattice" is quantized one can use a semiclassical approach in view of the large energy separation of the molecular magnetic levels which prevents a direct scattering process with a nuclear Zeeman transition accompanied by a transition between adjacent molecular magnetic levels. In such a case the nuclear relaxation is due to the lifetime broadening of the magnetic states which generates a randomly fluctuating local field arising from the hyperfine interaction of the nuclei with the electronic spins. In this case, $1/T_1$ and $1/T_2$ can be simply expressed in terms of the correlation function of a randomly time dependent perturbation term $\mathcal{H}_1$ (smaller than the nuclear Zeeman energy) in the Hamiltonian representing the nuclear-electron coupled system,[42,43]

$$\frac{1}{T_1} = \mathcal{J}_\perp(\omega_L) = \frac{2}{\hbar^2} \int_{-\infty}^{+\infty} \langle \mathcal{H}_1^\perp(t) \mathcal{H}_1^\perp(0) \rangle e^{-i\omega_L t} dt, \quad (3)$$

$$\frac{1}{T_2} = \mathcal{J}_z(0) + \frac{1}{2T_1} = \frac{2}{\hbar^2} \int_{-\infty}^{+\infty} \langle \mathcal{H}_1^z(t) \mathcal{H}_1^z(0) \rangle dt + \frac{1}{2T_1}, \quad (4)$$

where ω_L is the nuclear Larmor frequency and $\mathcal{J}_\alpha(\omega)$ are spectral densities of longitudinal ($\alpha = z$) and transverse ($\alpha = \perp$) components of the fluctuating local field. It is noted that Eqs. (3) and (4) are valid in the weak collision limit in which one assumes that the correlation time is much shorter than the relaxation time so that many elementary processes of fluctuations are required to induce a transition in the stationary nuclear Zeeman energy levels. In Eq. (4), we neglect the contribution due to rigid lattice nuclear dipolar interaction and we assume the fast motion regime, i.e., the fluctuations of the local hyperfine field are fast with respect to the interaction frequency itself.[43] Since each ^{57}Fe nucleus is dominated by the contact hyperfine interaction with the ionic spin of the Fe^{3+} ion to which the nucleus belongs, one has

$$\mathcal{H}_1 = A\mathbf{I} \cdot \mathbf{S} = A[I_z S_z + 1/2(I_+ S_+ + I_- S_-)] = \gamma_N \hbar (I_z H_z + I_\perp H_\perp), \quad (5)$$

where we have introduced the local effective hyperfine field H_α ($\alpha = z, \perp$) and γ_N is the nuclear gyromagnetic ratio. Under the assumption of an exponential decay of the correlation function of the hyperfine field, one has from Eqs. (3)–(5),

$$\frac{1}{T_1} = \gamma_N^2 \langle \Delta H_\perp^2 \rangle \frac{\tau_c}{1 + \omega_L^2 \tau_c^2}, \quad (6)$$

$$\frac{1}{T_2} = \gamma_N^2 \langle \Delta H_z^2 \rangle \tau_c, \quad (7)$$

where $\langle \Delta H_\perp^2 \rangle = A_\perp^2 \langle S_\perp^2 \rangle$ and $\langle \Delta H_z^2 \rangle = A_z^2 \langle S_z^2 \rangle$ and we neglected the second term in Eq. (4) since $T_2 \ll T_1$.

In the low temperature region, the fluctuations of the local hyperfine field are due to the transitions among the low lying m magnetic states. For temperatures below 2 K where our measurements were performed, one can make the assumption that the fluctuating field is due to random jumps between two values of the hyperfine field[43,44] corresponding to the $m = \pm 10$ and $m = \pm 9$ states as shown by Goto *et al.* in Mn12.[45] In this model one can assume a two-state pulse fluctuation with the magnitude h_α of the random field jumps and lifetimes τ_0 and τ_1, respectively, for the two states. The average fluctuating field between the two field values $H_1 = \tau_0 h_\alpha/(\tau_0 + \tau_1)$ and $H_2 = -\tau_1 h_\alpha/(\tau_0 + \tau_1)$ can be written as $\langle \Delta H_\alpha(t) \rangle = \tau_1 h_\alpha/(\tau_0 + \tau_1)$.

Utilizing the detailed balance condition for the transition probabilities and some algebra, one can derive $\langle \Delta H_\alpha^2 \rangle$ and τ_c to be used in Eqs. (6) and (7),

$$\langle \Delta H_\alpha^2 \rangle = \frac{\tau_0 \tau_1}{(\tau_0 + \tau_1)^2} h_\alpha^2 \approx \frac{\tau_1}{\tau_0} h_\alpha^2, \quad (8)$$

$$\tau_c = \frac{\tau_0 \tau_1}{\tau_0 + \tau_1} \approx \tau_1, \quad (9)$$

where we used the fact that $\tau_0 = \tau_{-10} \gg \tau_1 = \tau_{-9}$. The lifetimes $\tau_0 = \tau_{-10}$ and $\tau_1 = \tau_{-9}$ can be obtained from the spin-phonon transition probabilities,[46]

$$\frac{1}{\tau_m} = W_{m \to m+1} + W_{m \to m-1}, \quad (10)$$

with

$$W_{m \to m \pm 1} = \mathcal{C} s_{\pm 1} \frac{(E_{m \pm 1} - E_m)^3}{\exp[(E_{m \pm 1} - E_m)/T] - 1},$$

where $s_{\pm 1} = (s \mp m)(s \pm m + 1)(2m \pm 1)^2$ and the spin-phonon coupling parameter, $\mathcal{C}$, will be assumed to be the same as derived from proton relaxation in Fe8.[27]

Finally, the forms of $1/T_1$ and $1/T_2$ are simplified as

$$\left(\frac{1}{T_1} \right)_{sp} = \frac{(\gamma_N h_\perp)^2}{\tau_0} \frac{\tau_1^2}{1 + \omega_L^2 \tau_1^2}, \quad (11)$$

$$\left(\frac{1}{T_2} \right)_{sp} = (\gamma_N h_z)^2 \frac{\tau_1^2}{\tau_0}. \quad (12)$$

In this simple model both $1/T_1$ and $1/T_2$ are determined by the known lifetimes of two lowest mth magnetic levels and by the amplitude of fluctuating field, h_α which is the only fitting parameter.

A more general formula for $1/T_2$ had been obtained by Kohmoto *et al.*[44] using a nonlinear theory of phase relaxation in the pulse fluctuating field instead of using the correlation function. We just present the result of the theory without derivation,

$$\frac{1}{T_2} = \frac{1}{\tau_0} \frac{(\gamma_N h_z \tau_1)^2}{1 + (\gamma_N h_z \tau_1)^2}. \tag{13}$$

In the fast motion regime $(\gamma_N h_z \tau_1)^2 \ll 1$ the above formula becomes equivalent to Eq. (12). In the slow motion regime $(\gamma_N h_z \tau_1)^2 \gg 1$, it leads to

$$\frac{1}{T_2} = \frac{1}{\tau_0}, \tag{14}$$

which is identical to the result obtained in the strong collision regime as shown in the following.

B. Nuclear relaxation due to quantum tunneling

At low temperature the quantum tunneling of the magnetization (QTM) becomes an important factor in determining the spin dynamics in Fe8 nanomagnet. At very low temperature the tunneling takes place in the ground state $m = \pm 10$ (pure quantum tunneling regime) while at higher temperatures the tunneling can occur in the higher energy states, i.e., $m = \pm 9$, $m = \pm 8$, which are thermally populated by spin-phonon transitions (phonon assisted tunneling regime). Since the transverse terms in the Hamiltonian Eq. (1), which are responsible for the tunneling splitting Δ, are normally much smaller than the decoherence effects which generate the level broadening δ only incoherent tunneling is expected to occur in the temperature range of our experiments (0.05–1.5 K). We define here an incoherent effective tunneling probability Γ as the probability per unit time that a molecule reverses the direction of its magnetization (with respect to the easy axis) as a result of a tunneling transition with exchange of energy with the thermal bath (phonons, nuclei). Since time dependence of the orientation of the magnetization of the molecule generates a fluctuating hyperfine field at the nearby nuclei an additional contribution to nuclear relaxation associated with the tunneling dynamics is expected. Two very different scenario's are possible. If the NMR experiment is performed in a strong external magnetic field then the change of hyperfine field due to tunneling can be a small perturbation of the nuclear Zeeman energy and the perturbative weak collision approach can still be used. In this case the tunneling contribution to relaxation can be described by a simple expression of the form

$$\left(\frac{1}{T_1}\right)_T \quad \text{or} \quad \left(\frac{1}{T_2}\right)_T = A_\alpha^2 \frac{2\Gamma}{\Gamma^2 + \omega_L^2}, \tag{15}$$

where A_α ($\alpha = z$ or $\perp$) is the average fluctuating hyperfine field due to the magnetization reversal when a tunneling transition occurs, ω_L is the nuclear Larmor frequency, and Γ is the effective tunneling probability defined above. An expression of the form Eq. (15) was indeed found to explain the proton relaxation data in Fe8 when the proton NMR is observed in an external magnetic field.[25]

On the other hand, in the case of [57]Fe NMR in zero field or in low fields as well as proton NMR in zero field the change of local field due to a tunneling event cannot be treated as a small perturbation. In fact a tunneling transition between pairwise degenerate states, $\pm m$, results in the sudden inversion of the quantization axis for the nucleus. In this case a sudden approximation strong collision approach should be utilized to describe the nuclear spin-lattice relaxation rate. The nuclear relaxation by strong collision has been treated in details in the case of quadrupole relaxation by a sudden change of the quantization axis as the result of molecular reorientation.[47] It has also been discussed in the special case of relaxation in the rotating frame for modulation of the nuclear dipolar interaction by ultra slow diffusional motion in insulators.[48,49] In the present case the situation is well described by a strong collision due to the rapid inversion of the magnetic field direction.[50] Since the tunneling event occurs in a time much shorter than the inverse of the nuclear Larmor frequency a nonadiabatic approach is applicable[47] and one obtains that the nuclear relaxation transition probability W is practically the same as the tunneling transition probability Γ defined above, i.e.,

$$\left(\frac{1}{T_1}\right)_T \quad \text{or} \quad \left(\frac{1}{T_2}\right)_T = 2W = c(2\Gamma), \tag{16}$$

where c is a constant of the order of one and Γ is the effective incoherent tunneling rate. A derivation of Eq. (16) from a master equation approach is given in the Appendix.

It is noted that for $1/T_2$, Eq. (16) is indeed the same as Eq. (14) obtained in the slow motion regime. Also the strong collision result Eq. (16) can be formally derived form Eq. (15) in the limit of slow motion ($\Gamma \gg \omega_L$) when $A_\alpha \approx \omega_L$.

VI. ANALYSIS OF THE EXPERIMENTAL RESULTS FOR NUCLEAR RELAXATION RATES

A. Spin-lattice relaxation rate ($1/T_1$)

1. [57]Fe results in zero field and small longitudinal magnetic fields

The temperature dependence of the [57]Fe $1/T_1$ in zero external magnetic field is plotted in Fig. 4. The main feature here is the T-independent plateau reached below 0.4 K, the same temperature at which the quantum tunneling regime is observed in magnetization measurements.[12] In Fig. 5 we show the field dependence at 1.35 K of the [57]Fe $1/T_1$ in oriented powder with the magnetic field applied along the main anisotropy axis z. The main feature in this case is the sudden drop of the relaxation rate when a small longitudinal field is applied. Again, this is a clear indication of the presence of a contribution to relaxation due to quantum fluctuations since the contribution is removed by the small longitudinal field which prevents quantum tunneling to occur.

In order to support our claim that the nuclear relaxation rate is the direct measurement of the tunneling rate we estimate the latter on the basis of existing theories and experimental results, and compare it to $1/T_1$.

The incoherent tunneling probability can be written as[46,51,52]

$$\Gamma_{m,m'} = \frac{\Delta_{m,m'}^2 W_m}{(\xi + \Delta E_{m,-m})^2 + W_m^2}. \tag{17}$$

$\Delta_{m,m'}$ represents the tunneling splitting of the corresponding m states. W_m is a broadening parameter of the magnetic m
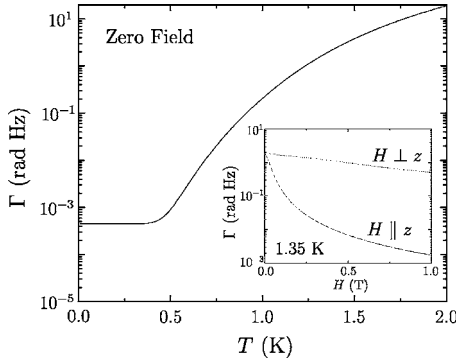
FIG. 10. Calculated tunneling probability Γ versus T plot. In inset, Γ is plotted against H_z (solid line) and $H_\perp$ with the tilting angle, $\theta=3°$ (dotted line) at 1.35 K.

state which includes both the lifetime broadening due to spin-phonon interaction and the hyperfine interaction with nuclei, and ξ is the longitudinal component of the internal bias field due to intermolecular dipolar interaction. Finally, $\Delta E_{m,m'}$ represents the external bias due to the application of a longitudinal field which splits the otherwise degenerate m states.[53] The measured quantity is the effective tunneling rate obtained by summing the tunneling probability for the different m states weighted by the corresponding Boltzmann facto,

$$\Gamma = \sum_m \Gamma_{m,m'} \exp(-E_m/k_B T). \quad (18)$$

The tunneling splittings necessary to calculate Γ from Eqs. (17) and (18) can be calculated from the model Hamiltonian with the fourth order correction terms,

$$\mathcal{H} = DS_z^2 + E(S_x^2 - S_y^2) + g\mu_B \mathbf{S} \cdot \mathbf{H} + D_2 S_z^4 + E_2[S_z^2(S_x^2 - S_y^2)$$
$$+ (S_x^2 - S_y^2)S_z^2] + C(S_+^4 + S_-^4). \quad (19)$$

The tunneling splitting in the ground state was measured directly with Landau-Zener tunneling experiments and found to be $\Delta_{10} \sim 10^{-7}$ K.[12] Thus we use in Eq. (19) the values of the parameters $D = -0.293$ K, $E = 0.047$ K, $D_2 = 3.54 \times 10^{-5}$ K, $E_2 = 2.03 \times 10^{-7}$ K from Ref. 38 but for C we use a different value, i.e., $C = -2.7 \times 10^{-5}$ K so as to obtain agreement with the experimental value of Δ_{10}. Then by solving Eq. (19) we find $\Delta_{10} = 0.5 \times 10^{-7}$ K, $\Delta_9 = 3.6 \times 10^{-6}$ K, and $\Delta_8 = 1.3 \times 10^{-4}$ K. With the values of Δ_m calculated above inserted in Eqs. (17) and (18) one explains both the field dependence in Fig. 5 and the T dependence in Fig. 4 with a choice of fitting parameter $W_{10} = 2.5 \times 10^8$ (rad Hz), $W_9 = 7 \times 10^9$ (rad Hz), and $W_8 = 9 \times 10^{10}$ (rad Hz). The parameter ξ in Eq. (17) was set $\xi = 4.4 \times 10^9$ (rad Hz) corresponding to the correct order of magnitude for intermolecular dipolar fields.[54,55] The broadening parameter W_{10} for the ground state is in good agreement with the value measured directly by "hole digging" experiments.[55] The rapid increase of the broadening parameter W_m for m smaller than 10 is consistent with the rapid increase of the density of states of phonons, which contribute to W_m at higher temperatures. The T and H dependences of Γ calculated from the parameters given above are shown in Fig. 10. We thus conclude that our

measured Γ is consistent with the tunneling splitting Δ_{10} and the broadening W_{10} obtained from theory and different experiments. We emphasize once more that NMR measures directly the incoherent tunneling rate Γ while the consistency with known values of the tunneling splitting is based on Eq. (17) and is thus indirect. In principle the tunneling rate Γ deduced from $1/T_1$ under the assumption of Eq. (16) should be directly comparable to the relaxation rate of the magnetization measured with the SQUID. As a matter of fact, a value of $\Gamma = 0.5 \times 10^{-3}$ s can be inferred at 50 mK from Landau-Zener tunneling experiments[13] in perfect agreement with our result of $1/T_1 = 2\Gamma$ in Fig. 4. Other SQUID measurements in the literature, although of the same order of magnitude as ours, are more difficult to compare with the NMR results either because they were performed in nonzero external field or because the relaxation of the magnetization was strongly nonexponential and only the initial decay of the magnetization was analyzed with a square root of t time dependence.[5,54,55]

2. ^{57}Fe *results in transverse magnetic field*

The transverse field dependence of $1/T_1$ is shown in Fig. 6. Contrary to the case of the H_z dependence, $1/T_1$ increases rapidly with increasing $H_\perp$. The spin-phonon contribution calculated by Eq. (11) appears to be very long compared to the experimental data, and weakly field dependent (dashed line in Fig. 6). Thus we may think that QTM is responsible for the fast increase of $1/T_1$ because Δ_m is expected to increase exponentially in an applied transverse field as calculated from the model Hamiltonian. However, the tunneling contribution given by Eq. (15) with the same parameters used in the H_z dependence of $1/T_1$ increases too fast leading to the wrong fit of the data above 0.2 T (dotted line in Fig. 6).

One may ask why the tunneling contribution predicted by the theory cannot be detected in the experiments. The answer could be given by the consideration of the fact that our sample is aligned powder so that it would be difficult to estimate the transverse field dependence of Δ_m due to the distribution of molecules in the xy plane, and/or a small misalignment of the sample may greatly reduce the tunneling contribution. We argue that the tunneling effect on the relaxation rate $1/T_1$ can be quenched by the presence of a small longitudinal component of the field. In fact, it was found, by proton NMR in Fe8 single crystal, that the tilting of 5° between the applied field and the xy plane eliminates the tunneling effects.[25] In our measurements, the possibility of the misalignment of the sample at least up to 5° should be taken into account. If so, it would be difficult to observe the increase of $1/T_1$ due to the tunneling contribution. In order to verify this argument, we simulated the situation in which the sample is misaligned by 3° off xy plane on the assumption of the azimuthal angle $\phi = 45°$. As it is clearly seen in Fig. 11, the degeneracies between $\pm m$ level pairs at zero field, which are preserved without tiling angle [Fig. 11(a)], are removed immediately by applying the transverse field for the misalignment of 3° [Fig. 11(b)]. It means that the energy difference between $\pm m$ levels cannot be treated as the tunnel splitting because $\pm m$ levels are no longer degenerate states in the
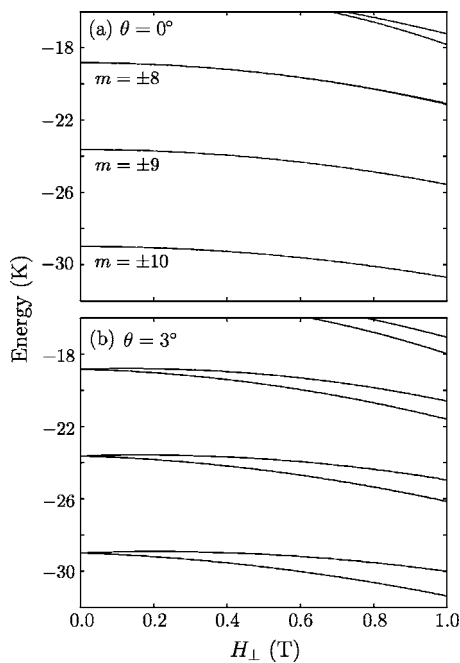
FIG. 11. Energy level diagrams of three lowest $\pm m$ pairs in an applied transverse field (a) with no tilting (b) with a tilting angle, $\theta = 3°$. It is evident that a small misalignment of the sample off xy plane removes the degeneracy of $\pm m$ sublevels.

tilted "transverse" field. It should be emphasized that this situation is also true for a tiny misalignment, for example, 0.5°. Therefore, the predicted fast increase of Δ_m with a transverse field does not take place in presence of an even small misalignment of the sample.

When a transverse external field is applied, however, we should consider "canting effect." In the presence of a transverse field, the direction of the internal local field, $|\mathbf{H}_{int}|$, is canted from the easy axis[56,57] by $\theta = \sin^{-1}(M_\perp/M_s)$, where $M_\perp$ is the transverse magnetization and M_s is the saturation magnetization of the $S = 10$ ground state. The length of the effective magnetic field is given by $|\mathbf{H}_{eff}| = |\mathbf{H}_{int} + \mathbf{H}_{ext}| = \sqrt{H_{int}^2 + H_{ext}^2 + 2H_{int}H_{ext}\sin\theta}$. The transverse components of the fluctuation of the local field generated by canting of the magnetization could be very efficient for the spin-lattice relaxation process. Consequently $1/T_1$ due to canting effect should be added to the spin-phonon and the tunneling contributions,

$$\frac{1}{T_1} = \left(\frac{1}{T_1}\right)_{cant} + \left(\frac{1}{T_1}\right)_{sp} + \left(\frac{1}{T_1}\right)_T. \qquad (20)$$

In presence of canting of the magnetization the transverse components of the hyperfine field are proportional to $\sin\Theta$ where Θ is the angle between $\mathbf{H}_{eff}$ and $\mathbf{H}_{int}$. The angle can be estimated from the field dependence of the NMR spectral line and using the relation $\Theta = \cos^{-1}[(H_{eff}^2 + H_{int}^2 - H_{ext}^2)/2H_{eff}H_{int}]$.[57] Here we assume that $(1/T_1)_{cant}$ can be obtained replacing $\gamma_N h_\perp$ in Eq. (11) with $\alpha\sin\Theta$ where $\alpha = 4.1 \times 10^8$ (rad Hz) is chosen in order to fit the data. The agreement between the data and the theory, as it is shown with the solid line in Fig. 6, is very good except for the small

deviations at low fields. Therefore, one concludes that for the $H_\perp$ dependence of $1/T_1$, $(1/T_1)_{cant} \gg (1/T_1)_{sp} + (1/T_1)_T$.

B. Spin-spin relaxation rate ($1/T_2$)

1. ⁵⁷Fe magnetic field dependence of $1/T_2$

The longitudinal and transverse field dependences of $1/T_2$ are shown in Fig. 7. In the longitudinal field, $1/T_2$ decreases at a moderate rate with increasing H_z, while it is almost constant in the transverse field. $1/T_2$ in both directions can be fitted by Eq. (12) with $\gamma_N h_z = 2 \times 10^7$ (rad Hz). The tunneling contribution calculated from Eq. (16) is negligible so that the spin-phonon contribution is dominant for $1/T_2$. Also it turns out that the canting of the magnetization has no effect on the transverse field dependence of $1/T_2$ due to the fact that it affects only the transverse component of the fluctuation of the magnetization.

2. ⁵⁷Fe temperature dependence of $1/T_2$

For the temperature dependence of $1/T_2$, the data is fitted well above 1 K with Eq. (12), but it starts to deviate below 1 K as shown in Fig. 8. The discrepancy between the data and the theoretical curve can be resolved by adding the constant value of 1.6×10^3 s. Thus, $1/T_2$ seems to level off at a constant value, as in the case of $1/T_1$. However, the origin of the leveling-off of $1/T_2$ cannot be the tunneling dynamics because its contribution from Eq. (16) is negligible at all temperatures. We argue below that the constant value of $1/T_2$ for $T \to 0$, i.e., 1.6×10^3 s arises from the nuclear dipolar interaction mostly between ⁵⁷Fe and ¹H nuclei.

The irreversible decay of the transverse magnetization (i.e., T_2 process) due to the nuclear dipolar interaction may originate from two contributions: (i) the dipolar interaction between like nuclei, (ii) the fluctuation of the dipolar fields arising from unlike nuclei. The order of magnitude of these contributions can be estimated from the calculation of the Van Vleck second moments.[58] For ⁵⁷Fe NMR in Fe8, (i) should be negligible because the second moment M_2 due to ⁵⁷Fe nuclei is estimated to be of the order of 7×10^2 s⁻², which is four orders of magnitude smaller than $M_2 \sim 1.6 \times 10^7$ s⁻² for ⁵⁷Fe−¹H dipolar interaction. Then, the contribution (ii) must be the dominant one. In the weak collision fast motion approximation one can express $1/T_2$ in terms of the spectral density at zero frequency, $J_z(0)$, of the fluctuations of the hyperfine field. Since in the present case the hyperfine field is the dipolar interaction due to the ¹H nuclear moments at the ⁵⁷Fe site one can write $1/T_2 \approx M_2 J^0(0) \approx M_2\tau_c$, where τ_c is a correlation time and M_2 is the second moment[58] of the ¹H−⁵⁷Fe dipolar interaction. We should point out that the formula mentioned above has the same form as Eq. (7), and so it is valid only in the fast motion regime, i.e., $\sqrt{M_2}\tau_c \ll 1$. If we identify τ_c with the proton T_2 value ($\sim 10^{-3}$ s) measured at low temperatures[26] then $\sqrt{M_2}\tau_c = 4$ indicating that the fast motion approximation is not applicable. Then one must refer to the quasistatic approximation whereby the effect on the relaxation of the ⁵⁷Fe nuclear transverse magnetization arises from the dephasing of the Hahn echo due to the slow fluctuations of the ⁵⁷Fe−¹H

dipolar interaction.[59] By using the line narrowing approach in the nearly static regime one has that the contribution to the decay of the echo signal can be expressed approximately as[59]

$$1/T_2^{\text{eff}} = \left(\frac{M_2}{12\tau_c} \right)^{1/3}.$$ (21)

With the values quoted above for M_2 and τ_c one has $1/T_2^{\text{eff}} = 1.1 \times 10^3$ s^{-1} in excellent agreement with the low T limiting value of ^{57}Fe $1/T_2$ of 1.6×10^3 s^{-1}. It is noted that strictly speaking the decay of the echo signal in the nearly static regime is not exponential.[59] In our case the detailed study of the form of the decay curve of the transverse magnetization is prevented by the weakness of the NMR signal. However, the above discussion of the orders of magnitude remains valid.

C. Comparison of ^{57}Fe relaxation rate in Fe8 with ^{1}H relaxation in Fe8 and ^{55}Mn relaxation in Mn12

On the basis of Eq. (16) we have argued that the measured $1/T_1$ in Fig. 4 is a direct measurement of the incoherent tunneling rate Γ. It is instructive to observe that the strong collision result [Eq. (16)] can be obtained as a limit of the weak collision result, Eq. (15). In the limit of slow motion ($\Gamma \ll \omega_L$) and for the case of a total change of local field, i.e., $A_\alpha \cong \omega_L$, Eq. (15) does indeed reduce to the strong collision case Eq. (18). For the case of ^{57}Fe NMR the local hyperfine field is directed along the magnetization of the molecule and a tunneling event corresponds to a simple reversal of the direction of the quantization field for the nucleus detected. Thus one may argue that $A_\alpha = \omega_L$ in Eq. (15) and thus in the slow motion, strong collision limit Eq. (16) and Eq. (15) coincide for $c = 1$. On the other hand, for ^{1}H NMR a tunneling event corresponds to a change of both longitudinal and transverse components of the local hyperfine field at the proton site. Also each tunneling event affects the direction of the quantization axis of several protons close to the Fe^{3+} moments. These effects may lead to a constant c in Eq. (16) much bigger than one. The theoretical estimate of the constant c for the case of protons NMR in zero field is outside the scope of this paper and thus we treat c as an adjustable parameter in the fit of the proton data.

We compare now the results for ^{57}Fe NMR with our data for ^{1}H NMR in Fig. 9. Proton relaxation data in zero field have been published earlier[60] in non enriched Fe8. Our data in enriched ^{57}Fe8 show the same T dependence but are almost a factor of 2 larger which should be related to the nuclear spin isotope effect on the tunneling rate.[14] As can be seen the results for the T dependence of the proton relaxation in zero field track the ones for ^{57}Fe with a rescaling factor of the order of 10. This is consistent with the argument that the relaxation of both nuclei measure directly the effective tunneling rate Γ according to Eq. (16). The multiplication factor of 10 can arise from the value of the constant c in Eq. (16) which can be larger for ^{1}H NMR for the reasons discussed above.

Finally the ^{57}Fe relaxation data in Fe8 are compared in Fig. 12 with the ^{55}Mn relaxation data in Mn12 from Ref. 62. We emphasize that the Mn12 case is more complicate than
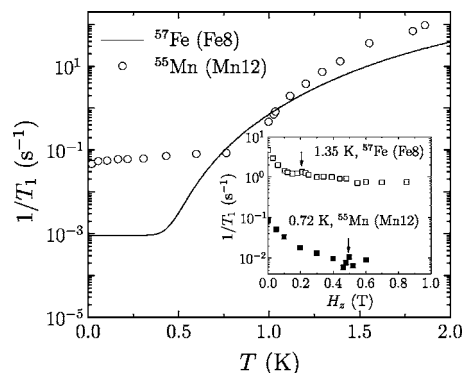
FIG. 12. Comparison of the temperature dependence of ^{57}Fe $1/T_1$ in Fe8 (full line) with ^{55}Mn $1/T_1$ in Mn12, extracted from Refs. 61 and 62. Inset shows the analogous comparison for the longitudinal field dependence. It is noted that as expected the small anomaly at the level crossing field both in Fe8 ($H_c \sim 0.22$ T) and Mn12 ($H_c \sim 0.5$ T) are observed at temperatures where the first excited states are thermally populated, and thermal assisted tunneling takes place.

Fe8. One could reinterpret the ^{55}Mn relaxation data in terms of strong collision with a caveat, the ^{55}Mn $1/T_1$ in Mn12 is dominated by the presence of a sizeable fraction of fast relaxing molecules combined with intercluster nuclear spin diffusion as shown in Refs. 61 and 62. Thus the low T plateau of $1/T_1$ in Mn12 should not be directly related to the tunneling rate of the bulk Mn12 sample but rather to a combination of the tunneling rate of the fast relaxing molecules and of the intercluster spin diffusion rate.

VII. SUMMARY AND CONCLUSIONS

A comprehensive ^{57}Fe NMR study has been carried out in order to investigate the static and dynamic magnetic properties in Fe8 molecular cluster. The temperature dependence of the resonance frequency in zero field is well explained in terms of the average total magnetic moment of the molecule which is reduced by thermal fluctuations as the temperature increases. The quantum tunneling of the magnetization (QTM) was detected by measuring the nuclear spin-lattice relaxation rates of ^{57}Fe as a function of the temperature and of longitudinal field. We argue that the tunneling contribution to $1/T_1$ in zero external magnetic field or small fields should be described in the framework of a strong collision theory. This leads to the remarkable result that at low fields and low T the relaxation rate is a direct measure of the tunneling rate. The direct measurement of the tunneling rate by NMR can be generalized to other molecules and should thus be a valuable tool to measure the tunneling rate in molecular nanomagnets under different experimental conditions. For the proper description of the tunneling effect, we propose a simple phenomenological model in terms of the tunneling probability that is determined by the tunnel splittings between pairwise degenerate $\pm m$ states. The experimental data are in good agreement with our theoretical calculations when both the thermal excitations due to spin-phonon interaction and the tunneling dynamics are included. For the spin-

phonon interaction we used values of the spin phonon coupling constant derived previously from proton NMR in Fe8. Regarding the tunneling effect we find that in order to fit the data one must assume a large fourth order term in the in-plane anisotropy of Fe8. This result is, however, consistent with previous observations reporting a tunneling splitting much larger than predicted on the basis of published values of the anisotropy constants and the fact that the ^{57}Fe isotopic enrichment increases the tunneling splitting. We compared our ^{57}Fe relaxation data in Fe8 to the ^{55}Mn relaxation in Mn12 to suggest that in the latter the nuclear relaxation data at very low T may also be reinterpreted in terms of a strong collision relaxation mechanism. When the magnetic field is applied perpendicular to the main easy axis we find the unexpected result that the tunneling dynamics does not contribute to the measured $1/T_1$. We demonstrate that the negligible tunneling effect in the transverse field is due to the breakdown of the degeneracy of $\pm m$ pairs by an inevitable tilting of the sample off the xy plane. Finally, it turns out that the tunneling dynamics gives no effect on both the temperature and field dependences of $1/T_2$ which can be explained in terms of ^{57}Fe–^{1}H nuclear dipolar interaction.

ACKNOWLEDGMENTS

APPENDIX: NUCLEAR RELAXATION IN THE STRONG COLLISION LIMIT

In most NMR measurements, the nuclear relaxation can be described by a perturbative approach (i.e., weak collision approach). It is obvious that the weak collision approximation is no longer valid if the local quantization field at the nuclear site reverses suddenly by, for example, the quantum tunneling of the magnetization.

This situation with a nuclear spin 1/2 is illustrated in Fig. 13. The two Hamiltonians are given by $\mathcal{H}_{a,b} = \gamma_n \mathbf{H}_{a,b} \cdot \mathbf{I}$ where $\mathbf{I}$ is the nuclear spin vector. The corresponding eigenstates are $|\pm\rangle_a$ and $|\mp\rangle_b$, respectively, and it is obvious that $|\pm\rangle_a = |\mp\rangle_b$. If the change of the local field is very fast compared to the nuclear Larmor frequency, i.e., $dH_{\text{loc}}/dt \cdot 1/H_{\text{loc}} \gg \omega_n = \gamma_n H_{\text{loc}}$, one may use the *sudden approximation*. In this case, since the nuclei (spin 1/2) cannot follow the change of the rapid reversal of the local field, the nuclear spin states cannot change, but the excited energy
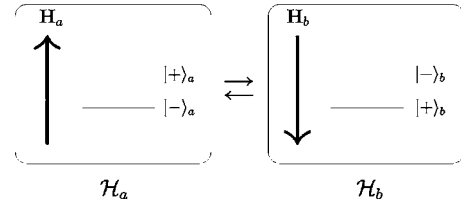
FIG. 13. The situation with a nuclear spin $\frac{1}{2}$.

state becomes ground state, and vice versa, after the jump of the local field. Therefore the populations in the two nuclear states must fulfill the following relation:

$$N_a^\pm = N_b^\mp. \tag{A1}$$

The rate equation for the populations for the Hamiltonian $\mathcal{H}_a$

$$\frac{dN_a^+}{dt} = W(|-\rangle_b \rightarrow |+\rangle_a)N_b^- - W(|+\rangle_a \rightarrow |-\rangle_b)N_a^+,$$

$$\frac{dN_a^-}{dt} = W(|+\rangle_b \rightarrow |-\rangle_a)N_b^+ - W(|-\rangle_a \rightarrow |+\rangle_b)N_a^-, \tag{A2}$$

where W denotes the transition rate. Also one can have similar equations for $\mathcal{H}_b$. It is easily seen that from Fig. 13 W's should be symmetric. Therefore,

$$W(|+\rangle_a \rightarrow |-\rangle_b) = W(|+\rangle_b \rightarrow |-\rangle_a) \equiv W^\pm,$$

$$W(|-\rangle_a \rightarrow |+\rangle_b) = W(|-\rangle_b \rightarrow |+\rangle_a) \equiv W^\mp. \tag{A3}$$

We assume now that the coupled system of nuclei and molecules are in thermal equilibrium with the lattice so that $W^\pm = W^\mp \exp(-\hbar\omega_n/k_B T)$. Since $\hbar\omega_n \ll k_B T$ at all accessible temperatures, i.e., the Boltzmann factor $e^{-\hbar\omega_n/k_B T} \sim 1$, one has in practice $W^\pm = \Gamma \approx W^\mp$ where Γ is the transition rate of the local field. From Eqs. (A2) and (A3), one can have

$$\frac{dM_a}{dt} = -2\Gamma(M_a - M_0),$$

$$\frac{dM_b}{dt} = -2\Gamma(M_b - M_0), \tag{A4}$$

where the magnetizations $M_{a,b}$ are given by the relationship $M_{a,b} = \gamma_n I(N_{a,b}^- - N_{a,b}^+)$, and M_0 is the equilibrium magnetization. Here we assumed that $M_a = M_b$.

Thus, in this simple model, the nuclear spin-lattice relaxation rate $1/T_1$ is equivalent to 2Γ, i.e., twice the transition rate of the local field,

$$\frac{1}{T_1} = 2\Gamma. \tag{A5}$$

*Present address: National High Magnetic Field Laboratory, Tallahassee, Florida, 32310.

[1] G. C. Papaefthymiou, Phys. Rev. B **46**, 10366 (1992).

[2] D. Gatteschi, A. Caneschi, L. Pardi, and R. Sessoli, Science **265**, 1054 (1994).

[3] *Magnetism: Molecules to Materials III*, edited by J. Miller and M. Drillon (Wiley-VCH, Weinheim, Germany, 2002).

[4] M. Leuenberger and D. Loss, Nature (London) **410**, 789 (2001).

[5] C. Sangregorio, T. Ohm, C. Paulsen, R. Sessoli, and D. Gatteschi, Phys. Rev. Lett. **78**, 4645 (1997).

[6] R. Sessoli, D. Gatteschi, A. Caneschi, and M. Novak, Nature (London) **365**, 141 (1993).

[7] L. Thomas, F. Lionti, R. Ballou, D. Gatteschi, R. Sessoli, and B. Barbara, Nature (London) **383**, 145 (1996).

[8] J. R. Friedman, M. P. Sarachik, J. Tejada, and R. Ziolo, Phys. Rev. Lett. **76**, 3830 (1996).

[9] E. Chudnovsky, Science **274**, 938 (1996).

[10] K. Wieghardt, K. Pohl, I. Jibril, and G. Huttner, Angew. Chem., Int. Ed. Engl. **23**, 77 (1984).

[11] M. Berry, Proc. R. Soc. London, Ser. A **392**, 45 (1984).

[12] W. Wernsdorfer and R. Sessoli, Science **284**, 133 (1999).

[13] W. Wernsdorfer, R. Sessoli, and D. Gatteschi, Europhys. Lett. **50**, 552 (2000).

[14] W. Wernsdorfer, A. Caneschi, R. Sessoli, D. Gatteschi, A. Cornia, V. Villar, and C. Paulsen, Phys. Rev. Lett. **84**, 2965 (2000).

[15] H. DeRaedt, S. Miyashita, K. Saito, D. Garcia-Pablos, and N. Garcia, Phys. Rev. B **56**, 11761 (1997).

[16] F. Hartmann-Boutron, P. Politi, and J. Villain, Int. J. Mod. Phys. B **10**, 2577 (1996).

[17] N. Prokof'ev and P. Stamp, J. Low Temp. Phys. **104**, 143 (1996).

[18] N. Prokof'ev and P. Stamp, Rep. Prog. Phys. **63**, 669 (2000).

[19] J. J. Alonso and J. F. Fernández, Phys. Rev. Lett. **87**, 097205 (2001).

[20] E. del Barco, N. Vernier, J. Hernandez, J. Tejada, E. Chudnovsky, E. Molins, and G. Bellessa, Europhys. Lett. **47**, 722 (1999).

[21] F. Luis, F. L. Mettes, J. Tejada, D. Gatteschi, and L. J. de Jongh, Phys. Rev. Lett. **85**, 4377 (2000).

[22] F. L. Mettes, F. Luis, and L. J. de Jongh, Phys. Rev. B **64**, 174411 (2001).

[23] E. del Barco, J. M. Hernandez, J. Tejada, N. Biskup, R. Achey, I. Rutel, N. Dalal, and J. Brooks, Phys. Rev. B **62**, 3018 (2000).

[24] L. Sorace, W. Wernsdorfer, C. Thirion, A.-L. Barra, M. Pacchioni, D. Mailly, and B. Barbara, Phys. Rev. B **68**, 220407(R) (2003).

[25] Y. Furukawa, K. Aizawa, K. Kumagai, R. Ullu, A. Lascialfari, and F. Borsa, Phys. Rev. B **69**, 14405 (2004).

[26] S. Maegawa and M. Ueda, Prog. Theor. Phys. Suppl. **145**, 380 (2002).

[27] Y. Furukawa, K. Kumagai, A. Lascialfari, S. Aldrovandi, F. Borsa, R. Sessoli, and D. Gatteschi, Phys. Rev. B **64**, 094439 (2001).

[28] M. Ueda, S. Maegawa, H. Miyasaka, and S. Kitagawa, J. Phys. Soc. Jpn. **70**, 3084 (2001).

[29] S. Baek, S. Kawakami, Y. Furukawa, B. Suh, F. Borsa, K. Kumagai, and A. Cornia, J. Magn. Magn. Mater. **272–276**, E771 (2004).

[30] Y. Furukawa, S. Kawakami, K. Kumagai, S. H. Baek, and F. Borsa, Phys. Rev. B **68**, 180405(R) (2003).

[31] C. Delfs, D. Gatteschi, L. Pardi, R. Sessoli, K. Wieghardt, and D. Hanke, Inorg. Chem. **32**, 3099 (1993).

[32] R. Watson and A. Freeman, Phys. Rev. **123**, 2027 (1961).

[33] P. Gütlich, in *Mössbauer Spectroscopy*, edited by U. Gonser (Springer-Verlag, Berlin, 1975).

[34] L. Cianchi, F. DelGiallo, G. Spina, W. Reiff, and A. Caneschi, Phys. Rev. B **65**, 064415 (2002).

[35] L. Walker, G. Wertheim, and V. Jaccarino, Phys. Rev. Lett. **6**, 98 (1961).

[36] The hyperfine coupling constant *A* depends on the electronic configuration and is thus insensitive to thermal effects unless a phase transition takes place.

[37] A.-L. Barra, D. Gatteschi, and R. Sessoli, Chem.-Eur. J. **6**, 1608 (2000).

[38] R. Caciuffo, G. Amoretti, A. Murani, R. Sessoli, A. Caneschi, and D. Gatteschi, Phys. Rev. Lett. **81**, 4744 (1998).

[39] C. Kittel, *Introduction to Solid State Physics* (Wiley, New York, 1996).

[40] The levels of $|m| < 5$ are strongly admixed, and thus the quantum number *m* loses any physical significance (Ref. 63). Conversely, this fact implies that the height of the energy barrier is not well defined.

[41] A theoretical approach to apply the *modified* spin wave theory has been attempted in Ref. 64. However, the application of the theory to Fe8 will be difficult due to complicated internal magnetic structure of Fe8 cluster.

[42] F. Borsa, in *Local Properties at Phase Transitions*, edited by K. Müller and A. Rigamonti (North-Holland, Amsterdam, 1976), p. 137.

[43] C. Slichter, *Principles of Magnetic Resonance* (Splinger-Verlag, Berlin, 1990).

[44] T. Kohmoto, T. Goto, S. Maegawa, N. Fujiwara, Y. Fukuda, M. Kunitomo, and M. Mekata, Phys. Rev. B **49**, 6028 (1994).

[45] T. Goto, T. Koshiba, T. Kubo, and K. Agawa, Phys. Rev. B **67**, 104408 (2003).

[46] M. N. Leuenberger and D. Loss, Phys. Rev. B **61**, 1286 (2000).

[47] S. Alexander and A. Tzalmona, Phys. Rev. **138**, A845 (1965), see also A. Rigamonti and J. R. Brookman, Phys. Rev. B **21**, 2681 (1980).

[48] C. Slichter and D. Ailion, Phys. Rev. **135**, A1099 (1964).

[49] D. Ailion and C. Slichter, Phys. Rev. **137**, A235 (1965).

[50] A hypothetical case of strong collision due to a rapid inversion of a magnetic field has been illustrated by A. Abragam, *The Principles of Nuclear Magnetism* (Clarendon, Oxford, 1961), pp. 477–479.

[51] A. Fort, A. Rettori, J. Villain, D. Gatteschi, and R. Sessoli, Phys. Rev. Lett. **80**, 612 (1998).

[52] I. Tupitsyn and B. Barbara, in *Magnetism: Molecules to Materials III*, edited by J. Miller and M. Drillon (Wiley-VCH, Weinhem, 2002).

[53] The expression to be used for the incoherent tunneling probability is still object of debate. The Eq. (17) used here is obtained by considering the effect of both a time independent bias field and a broadening of the levels. Thus Eq. (17) is obtained by integrating the expression for the coherent Rabi oscillation in a two level system which are not completely degenerate over a distribution of energy levels having a width *W* and an average energy difference given by $\xi + \Delta E_{m,-m}$. An alternative approach is to consider the incoherent tunneling as the result of a series of Landau-Zener tunneling events occurring every time the two levels cross as the result of a time dependent bias field $\xi(t)$ due to nuclear hyperfine interactions and/or intermolecular dipolar

interactions (see Ref. 54). It is noted that in both cases the qualitative result is similar, namely the tunneling probability per unit time $\Gamma_{m,m'}$ is strongly suppressed by the combination of both the broadening and the average bias field as shown in Eq. (17).

[54] N. V. Prokof'ev and P. C. E. Stamp, Phys. Rev. Lett. **80**, 5794 (1998).

[55] W. Wernsdorfer, T. Ohm, C. Sangregorio, R. Sessoli, D. Mailly, and C. Paulsen, Phys. Rev. Lett. **82**, 3903 (1999).

[56] O. Kahn, *Molecular Magnetism* (VCH, New York, 1993).

[57] Y. Furukawa, K. Watanabe, K. Kumagai, F. Borsa, T. Sasaki, N. Kobayashi, and D. Gatteschi, Phys. Rev. B **67**, 064426 (2003).

[58] J. V. Vleck, Phys. Rev. **74**, 1168 (1948).

[59] M. Takigawa and G. Saito, J. Phys. Soc. Jpn. **55**, 1233 (1986).

[60] M. Ueda, S. Maegawa, and S. Kitagawa, Phys. Rev. B **66**, 73309 (2002).

[61] A. Morello, O. Bakharev, H. Brom, and L. de Jongh, Polyhedron **22**, 1745 (2004).

[62] A. Morello, Ph.D. thesis, Leiden University, The Netherlands, 2004; cond-mat/0404049 (unpublished); also see A. Morello *et al.*, cond-mat/0403107 (unpublished).

[63] A.-L. Barra, F. Bencini, A. Caneschi, D. Gatteschi, C. Paulsen, C. Sangregorio, R. Sessoli, and L. Sorace, ChemPhysChem **2**, 523 (2001).

[64] H. Hori and S. Yamamoto, Phys. Rev. B **68**, 054409 (2003).